Full Energy Electron Cross Section With 1.05 GeV Beam

Sebouh Paul

June 30, 2016

1 Introduction

There are two goals in this analysis. The first goal is to measure the overall efficiency of HPS in finding full energy electrons as a function of scattering angle. The second is to measure the elastic form factor of tungsten, and compare our measurement with existing data and models. In addition to the runs we took using the tungsten target, we also took a calibration run (# 5779) using the carbon target. This run used only the singles triggers, and had a smaller prescale factor for the trigger than we used for the tungsten runs.

2 Outline of Procedure

My first step is to calculate the accepted cross section of the FEEs in the carbon run. I do this by first counting the number of events that pass certain cuts within each angular bin, and then dividing that by the spherical angle of those bins, and then by the prescaled luminosity of the run. Then, I divide this by a model of the cross section in order to get the efficiency of the detector.

Then, I calculate the accepted cross section of the tungsten by doing the same procedure with some of the tungsten runs. To correct for the inefficiency, I divide this by efficiency that I had calculated from the carbon run. I then divide this cross section by the Mott scatting formula to get the form factor of the tungsten nucleus. Finally, I fit the calculated form factor to a Fermi model.

3 Theoretical Model

There are two types of processes that produce FEE events. The most common type of reaction is elastic scattering off the nucleus. The other type is called quasi-elastic scattering, that is, where the electron elastically scatters off only one of the nucleons in the nucleus. In other electron-nucleus scattering experiments, it is possible to distinguish between these

two types of events using the difference in energy of the scattered electron due to nucleon or nuclear recoil; however, HPS does not have good enough energy resolution to make this distinction.

At very low energies ($q \ll \hbar c/R_{rms}$, where R_{rms} is the rms charge radius of the nucleus), the elastic cross section can be approximated using the Mott scattering cross section (Equation 1 below), which is an relativistic extension of the Rutherford scattering formula.

$$\left(\frac{d\sigma}{d\Omega}\right)_{Mott} = \frac{Z^2\alpha^2}{4E^2\sin^4\frac{\theta}{2}}\cos^2\frac{\theta}{2}\left(\frac{1}{1+\frac{2E}{M}\sin^2\frac{\theta}{2}}\right) \tag{1}$$

where E is the beam energy, M is the nucleus mass, θ is the scattering angle, and Z is the atomic number of the nucleus.

It should be noted that Equation 1 is only valid for very small energy transfer, and does not take into account the internal structure of the nucleus or nucleon. The more appropriate formula for the cross section for elastic scattering off a nucleus or a nucleon is

$$\frac{d\sigma}{d\Omega} = \left(\frac{d\sigma}{d\Omega}\right)_{Mott}\left|F(Q^2)\right|^2 \tag{2}$$

where $F(Q^2)$ is the elastic form factor, a function that describes the nucleus or nucleon's internal structure. The form factor is a function of the momentum transferred Q^2, which, for elastic scattering, is

$$Q^2 = 4E^2\sin^2\frac{\theta}{2}\left(1+\frac{2E}{M}\sin^2\frac{\theta}{2}\right)^{-1} \tag{3}$$

The elastic form factor $F(Q^2)$ is related to two other form factors, the electric form factor $G_E(Q^2)$ and the magnetic form factor $G_M(Q^2)$ via:

$$\left|F(Q^2)\right|^2 = \frac{G_E^2 + \frac{\tau}{\epsilon}G_M^2}{1+\tau} \tag{4}$$

where $\tau = \frac{Q^2}{4M}$ and $\epsilon = (1+2(1+\tau)\tan^2\frac{\theta}{2})^{-1}$ are kinematic factors. Since our experiment's geometric acceptance restricts us to small angles (¡ 160 mrad), and the mass of the nucleus is much greater than the beam energy, the value of τ is small, especially for elastic events. In nuclear elastic scattering, the difference between the electric and elastic form factors ($G_E(Q^2)$ and $F(Q^2)$) is negligible (about 0.02% at worst). In quasielastic scattering, however, τ can be as large as 0.03, and therefore I take both the electric and magnetic form factors into account.

The electric form factor is related to the electric charge density by a Fourier transformation:

$$F(Q^2) = \frac{4\pi}{q} \int_0^\infty r\rho(r)dr \tag{5}$$

In my model, I treat the nucleus as if it is a Fermi gas at the ground state, which implies that all nucleon momentum states up to the Fermi momentum (k_F) are occupied. The cross section of quasielastic scattering off an individual nucleon is then analogous to elastic scattering off a nucleus with a few modifications. First, the atomic number Z is replaced with one, and the nucleus's form factor is replaced with that of the nucleon. Additionally, the cross section off an individual nucleon is zero if the magnitude of the sum of the initial momentum of the nucleon $\mathbf{k}_i$ and the transferred momentum $\mathbf{q}$ is less than the Fermi momentum (since such a scattering would place it in an already occupied momentum state). Making these assumptions, it is therefore possible to calculate the fraction of the nucleons that are in this region of momentum space:

$$f(x) = \begin{cases} \frac{3x}{4} - \frac{x^3}{16}, & x < 2 \\ 1, & x \geq 2 \end{cases} \text{ where } x = \frac{|\mathbf{q}|}{k_F} \tag{6}$$

Therefore I approximate the quasi-elastic scattering cross section as the elastic scattering cross section off a free nucleon multiplied by $f(x)$.

For this analysis, I am using the Fermi momentum values from [1]. The listed Fermi momentum for carbon-12 is 220 ± 5 MeV. The Fermi momenta is not available for any of the tungsten isotopes, so I substituted in the value listed for ${}_{73}\mathrm{T}^{181}$, which is 265 ± 5 MeV.

The total cross section (quasielastic plus nuclear elastic) is then the sum of the contributions from the nucleus as a whole, and the individual nucleons:

$$\frac{d\sigma}{d\Omega} = \left(\frac{d\sigma}{d\Omega}\right)_{\text{nucleus}} + f(x)\left[Z\left(\frac{d\sigma}{d\Omega}\right)_{\text{proton}} + N\left(\frac{d\sigma}{d\Omega}\right)_{\text{neutron}}\right] \tag{7}$$

Figure 1 shows the predicted cross section with the carbon and tungsten targets as a fraction of the Mott formula (Equation 1)

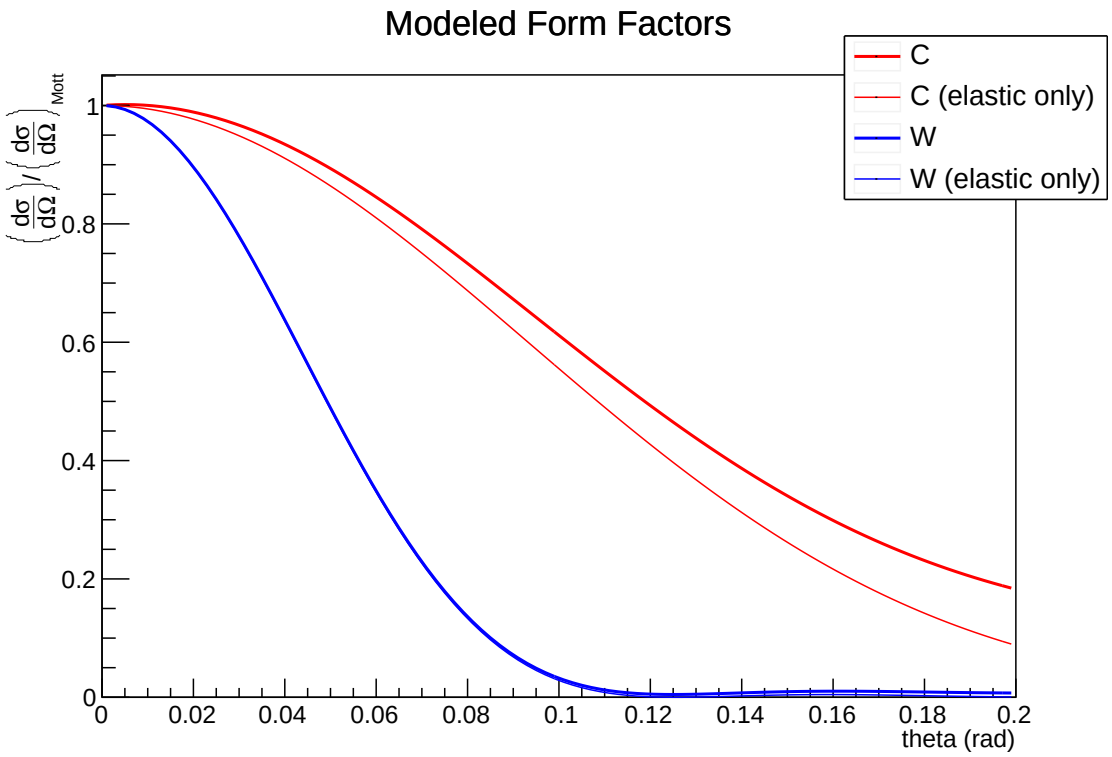

Figure 1: Theoretical Cross Sections. The thick red and blue curves represents the predicted cross sections per Mott for carbon and tungsten respectively. The thin curves of the same colors represent the elastic part of the predicted cross sections. The quasi-elastic contribution to the cross section for tungsten is very small compared to the elastic contribution, therefore the thin blue curve is hard to see against the thick blue curve.

3.1 Elastic Form Factors of Nucleons

In my treatment of the form factors of the nucleons in the quasielastic scattering, I followed J. J. Kelly's parameterizations in [2], which use rank [1/3] Pad approximants for three of the four form factors. The one exception is the neutron electric moment, G_{En}, for which there was not enough data available to accurately fit in the same manner. Therefore Kelly parameterized the ratio G_{En}/G_D, where G_D is the so-called standard dipole moment, $\left(1+\frac{Q^2}{.71*\mathrm{GeV}^2}\right)^{-2}$. Kelly's parameterizations of the electric and magnetic form factors for the proton and neutron are:

$$\begin{aligned} G_{Ep} =& \frac{1-.24\tau}{1+10.98\tau+12.82\tau^2+21.97\tau^3} \\ G_{Mp} =& \left(\frac{1+.12\tau}{1+10.97\tau+18.86\tau^2+6.55\tau^3}\right)\mu_p \\ G_{En} =& \left(\frac{1.7\tau}{1+3.3\tau}\right)\left(\frac{1}{1+\frac{Q^2}{.71*\mathrm{GeV}^2}}\right)^2 \\ G_{Mn} =& \left(\frac{1+2.33\tau}{1+14.72\tau+24.2\tau^2+84.1\tau^3}\right)\mu_n \end{aligned} \tag{8}$$

where μ_p and μ_n are the magnetic moments of the proton and neutron, 2.793 and -1.913 respectively. From these parameterizations, I use Equation 4 to calculate the elastic form factor $F(Q^2)$ of the nucleons.

3.2 Form Factors of Carbon

For the carbon form factor, i used the model independent parameterization from DeVries et al [3]. In this parameterization, they list the Fourier-Bessel coefficients a_i of the carbon nucleus, from which I calculate the form factor using the following expansion:

$$F(Q^2) = \sum_{i=1} a_i(-1)^{i+1} \frac{4\pi R^2 \hbar c \sin\frac{QR}{\hbar c}}{Q\left(i^2\pi^2 - \left(\frac{QR}{\hbar c}\right)^2\right)} \tag{9}$$

where R is an additional parameter, the cutoff radius, which in this case is 8 fm.

3.3 Form Factors of Tungsten

For the tungsten nucleus, I fit the measured elastic form factor to a Fermi model. In this model, the charge density (from which I calculate $F(Q^2)$ using Equation 5) is given by:

$$\rho(r) = \frac{\rho_0}{1 + \exp\frac{r-c}{z}} \tag{10}$$

In this case, the charge density is nearly constant until around R, and drops off to zero, with a drop-off width determined by c.

DeVries [3] lists the values of R and c as 6.51(7) and 0.535(36) fm for ^{184}W and 6.58(3) and 0.480(23) fm for ^{186}W, both of which were fit for q between 0.25 to .60 fm^{-1}. These values come from a fit made by Kalinsky et al [4] on data from an experiment at the Electron Accelerator Laboratory at Yale University in 1973. Similar information for other isotopes of tungsten is unavailable.

A variation of this model includes an additional parameter, w:

$$\rho = \frac{\rho_0(1 + w\frac{r^2}{R^2})}{1 + \exp\frac{r-c}{z}} \tag{11}$$

4 Runs Used In This Analysis

Obviously, we need to use run 5779 in this analysis, since it is the only run that uses the carbon target. For testing, I have been using run 5772 to look at the shape of the tungsten spectrum. At least, I will do so until I am ready to increase the statistics.

Note: At the low scattering angles (down to 40 mrad) there are almost 3 times as many events that pass the cuts in run 5779 than in 5772. This ratio increases to about 40 at large scattering angles (up to 160 mrad).

In the final version of this analysis, I plan to use all of the so called "golden runs", that is, the tungsten runs taken with the SVT at the 0.5 mm setting, with 50 nA beam and which have at least 5 million events in the run. When I increase my event sample, the number of events at large scattering angles should be commensurate in the tungsten and carbon runs.

5 Cuts

Since I am using the fee skim, the following cuts already exist in the data sample I am using:

- The trigger must be Single0 or Single1.
- There is a cluster in the event whose energy (prior to corrections) is at least 600 MeV, and the corrected energy of the most energetic hit (that is, the seed hit) is at least 400 MeV.

I found that it doesn't matter if I use the skim or the full data set, since the cuts I make cut out any event that wouldn't have passed the skim anyway.

I first required that the events use the Single1 trigger, and that all the event flags for the SVT status were good. I then look at the reconstructed particles collection data and make cuts on the clusters:

- The reconstructed cluster time is between 40 and 50 ns.
- The reconstructed energy of the cluster (after corrections) is between than 75% and 115% of the beam energy. (that is, between about 800 and 1200 GeV for a 1.056 GeV beam).
- The energy of the seed hit of the cluster is more than 38% of the beam energy (that is about 400 MeV for the 1.056 GeV beam).
- There are at least 3 hits in the cluster.

I then require that the cluster be matched to a track. The track must fulfill the following criteria:

- the track was fitted using the GBL algorithm.
- The track is negatively charged (curves to the right)
- Track momentum is between 75% and 115% of the beam energy (that is about 800 and 1200 MeV).
- The χ^2 value of the track fit is less than 50.
- The track's distance from the beamspot is less than 1 mm in the x direction, and less than 0.5 mm in the y direction.

If the track and the cluster fulfill these criteria, then I calculate theta and phi relative to the beam direction (.0295 mrad in the x direction and -.0008 mrad in the y direction). I fill a 2D histogram with the values of theta and phi..

I define a fiducial region in theta and phi in which I expect that the electron will hit the Ecal at least .75 crystals from the edge, and also will hit the sensitive region of the 5th layer of the SVT. Figure 2 shows the fiducial mask.

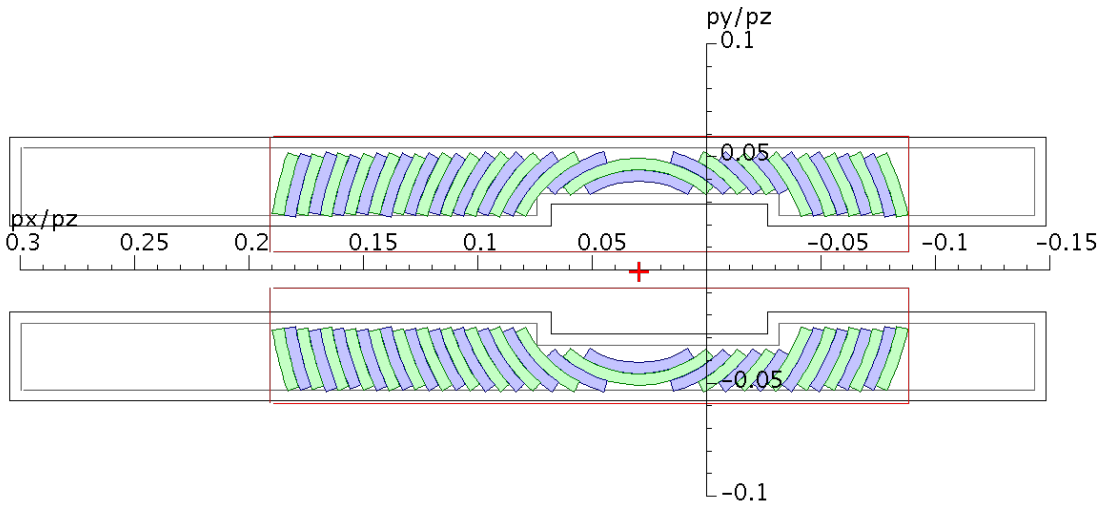

Figure 2: Fiducial mask. Each blue/green band represents 5 mrad insides of the fiducial region. Its edges are curves of constant theta and phi. The black outline represents the Ecal, and the grey outline inside it is .75 crystal widths from the edge. The red outline represents SVT layer 5. The red + sign represents the direction of the beam

6 Normalization

I get the charge of each run from the "total good Q at nominal (nC)" column of the run spreadsheet, on the page titled "golden runs." These numbers come from Sho's calculations using the SvtChargeIntegrator. This calculation includes only the charge accumulated when the bias is on, the position is at nominal, and takes into account the livetime correction.

The prescale factor p is 2^N, where N is a number specified in the trigger configuration file. For the tungsten runs, the prescale factor is $2^{11} = 2048$. For the carbon run, the prescale factor is $2^7 = 128$.

The measured areal densities ρ_A of the carbon and tungsten targets are 0.044 g/cm^2 and .0078 g/cm^2, respectively.

The prescaled luminosity is:

$$\ell = p\frac{\rho_A N_A}{A}\frac{Q}{q_e}\frac{1\text{ cm}^2}{10^{24}\text{ barn}} \tag{12}$$

Table 1 lists the prescaled luminosities of each of the runs used in the final analysis. These include all the runs with the tungsten target under normal conditions (SVT is 0.5 mm from the beamline; current is 50 nA; tungsten target is in place; and the run has at least 5 million events), as well as the carbon target run (5779).

Run #	prescale	A (amu)	ρ_A (g/cm^2)	charge (μC)	Prescaled lumi (μb^{-1})
5779	128	12.00	0.044	45.8	4935.5
5623	2048	183.84	0.0078	96.5	7.5
5624	2048	183.84	0.0078	62.5	4.9
5632	2048	183.84	0.0078	16.1	1.3
5634	2048	183.84	0.0078	121.7	9.5
5635	2048	183.84	0.0078	12.5	1.0
5636	2048	183.84	0.0078	28.2	2.2
5637	2048	183.84	0.0078	33.6	2.6
5642	2048	183.84	0.0078	97.4	7.6
5643	2048	183.84	0.0078	91.6	7.1
5644	2048	183.84	0.0078	102.7	8.0
5648	2048	183.84	0.0078	12.0	0.9
5649	2048	183.84	0.0078	38.6	3.0
5650	2048	183.84	0.0078	26.7	2.1
5651	2048	183.84	0.0078	12.9	1.0
5652	2048	183.84	0.0078	34.9	2.7
5653	2048	183.84	0.0078	18.8	1.5

Run #	prescale	A (amu)	ρ_A (g/cm^2)	charge (μC)	Prescaled lumi (μb^{-1})
5654	2048	183.84	0.0078	33.5	2.6
5655	2048	183.84	0.0078	7.0	0.5
5656	2048	183.84	0.0078	47.5	3.7
5657	2048	183.84	0.0078	9.3	0.7
5686	2048	183.84	0.0078	9.9	0.8
5689	2048	183.84	0.0078	140.3	10.9
5692	2048	183.84	0.0078	132.0	10.3
5693	2048	183.84	0.0078	157.1	12.2
5694	2048	183.84	0.0078	93.7	7.3
5695	2048	183.84	0.0078	46.3	3.6
5696	2048	183.84	0.0078	145.0	11.3
5697	2048	183.84	0.0078	29.6	2.3
5698	2048	183.84	0.0078	181.9	14.2
5704	2048	183.84	0.0078	2.7	0.2
5706	2048	183.84	0.0078	66.9	5.2
5710	2048	183.84	0.0078	56.0	4.4
5715	2048	183.84	0.0078	116.8	9.1
5723	2048	183.84	0.0078	240.7	18.7
5724	2048	183.84	0.0078	259.9	20.2
5725	2048	183.84	0.0078	192.2	15.0
5726	2048	183.84	0.0078	92.5	7.2
5733	2048	183.84	0.0078	20.4	1.6
5739	2048	183.84	0.0078	191.3	14.9
5741	2048	183.84	0.0078	219.1	17.1
5742	2048	183.84	0.0078	261.2	20.3
5743	2048	183.84	0.0078	135.3	10.5
5766	2048	183.84	0.0078	208.5	16.2
5768	2048	183.84	0.0078	198.1	15.4
5769	2048	183.84	0.0078	252.8	19.7
5770	2048	183.84	0.0078	276.2	21.5
5771	2048	183.84	0.0078	259.0	20.2
5772	2048	183.84	0.0078	264.9	20.6
5773	2048	183.84	0.0078	318.7	24.8
5775	2048	183.84	0.0078	124.3	9.7
5776	2048	183.84	0.0078	185.7	14.5
5782	2048	183.84	0.0078	274.6	21.4
5783	2048	183.84	0.0078	276.2	21.5
5791	2048	183.84	0.0078	229.7	17.9
5793	2048	183.84	0.0078	46.0	3.6

Run #	prescale	A (amu)	ρ_A (g/cm^2)	charge (μC)	Prescaled lumi (μb^{-1})
5795	2048	183.84	0.0078	194.9	15.2
5796	2048	183.84	0.0078	263.2	20.5
5797	2048	183.84	0.0078	219.7	17.1
			tungsten total	7287.5	567.5

Table 1: Luminosities of Runs used in FEE Analysis. These values are calculated using Equation 12

7 Scattering Angle

I calculate the scattering angle θ relative to the unit vector of the beam direction (.0295, -.0008, .9995). I obtained this direction using a simple analysis of Moller events, which deserves its own analysis note. However, I will briefly describe the procedure of this.

Due to the conservation of momentum, the sum of the momenta of the electrons in a moller event should be equal to the beam momentum. (There is some loss of momentum due to radiative effects, but this can be assumed to be very small) Therefore, the direction of the beam is the same as that of the vector sum of the electron momenta. Therefore I did a fit on the direction of the momentum sum vector, and got approximately (.0295, -.0008, .9995).

8 Results

8.1 Efficiency from carbon

Figure 3 shows the measured cross section for carbon within the fiducial region, compared to the predicted cross section, as a function of angle θ. I calculate the measured cross section by dividing the post-cuts event counts in each theta bin by the prescaled luminosity and fiducial solid angle of the bin.

Figures 4 and 5 show the calculated efficiency of the detector, that is, the ratio of the measured cross section to the predicted cross section, as a function of both theta and phi, and as a function of theta only (projected within the fiducial range in phi).

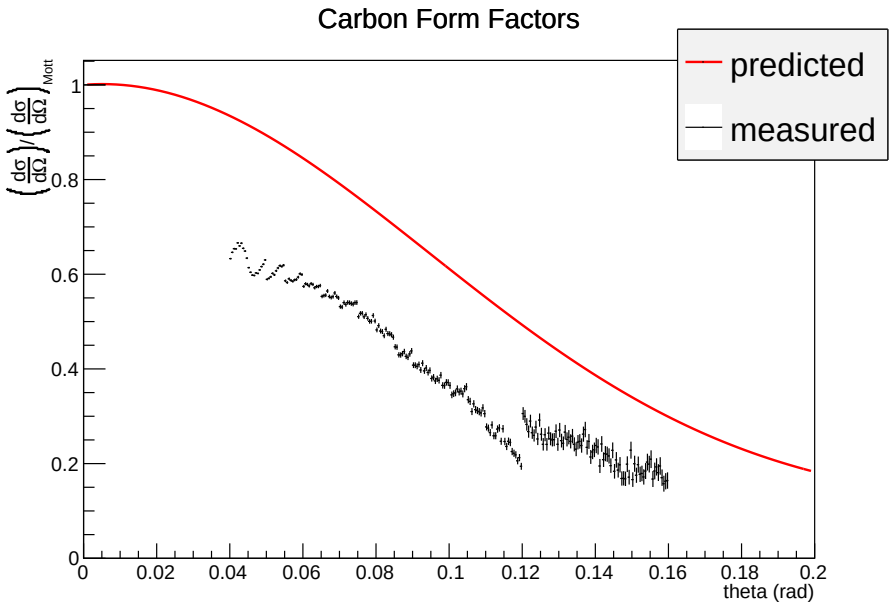

Figure 3: Measured vs predicted FEE cross sections with carbon target.

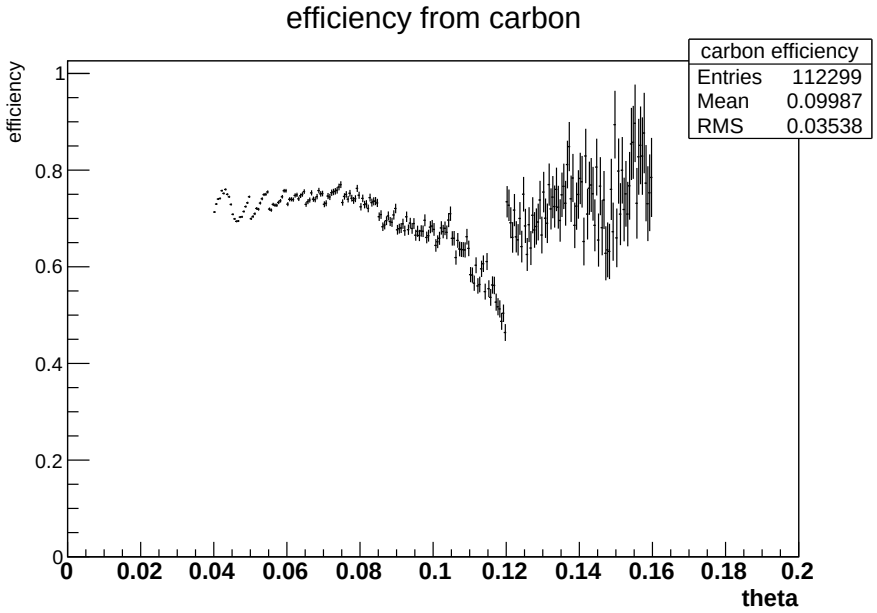

Figure 4: Efficiency of HPS for detecting FEEs as a function of theta and phi.

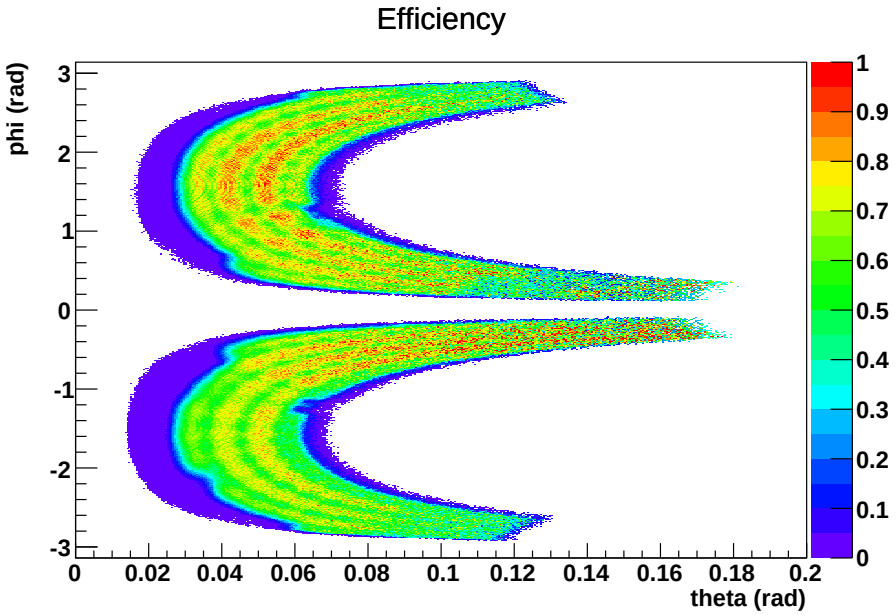

Figure 5: Efficiency of HPS for detecting FEEs as a function of theta. This is averaged over all values of ϕ in the fiducial range

8.2 Effects of Cuts

Each of the following histograms represents one or two variables that I am cutting on. The red lines represent the limits of the cut.

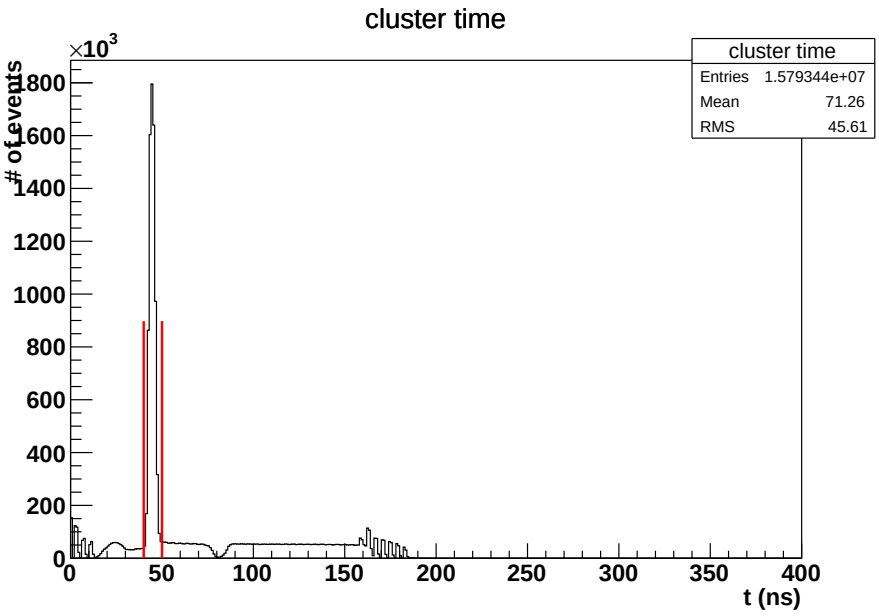

Figure 6: Cluster Time

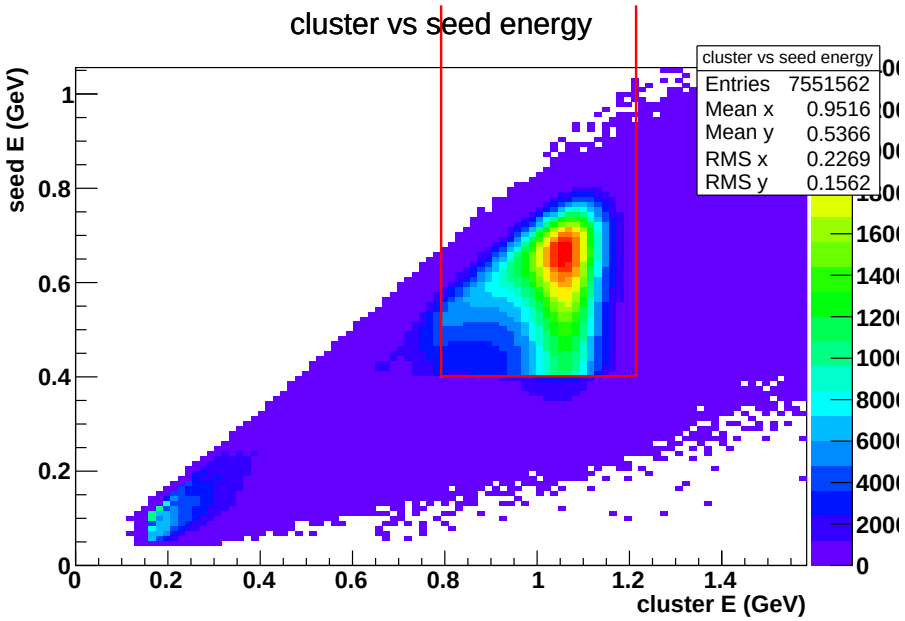

Figure 7: Cluster and Seed Energy

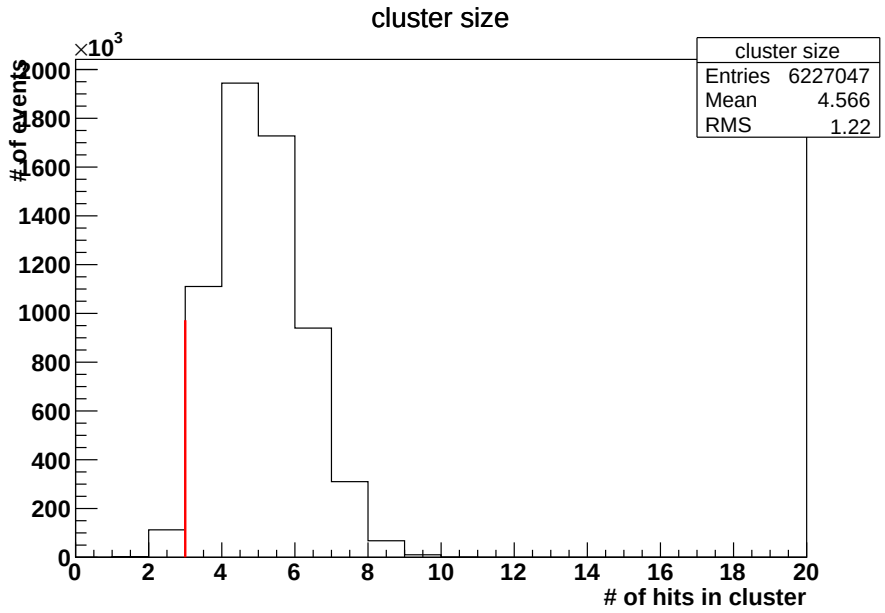

Figure 8: Cluster Size

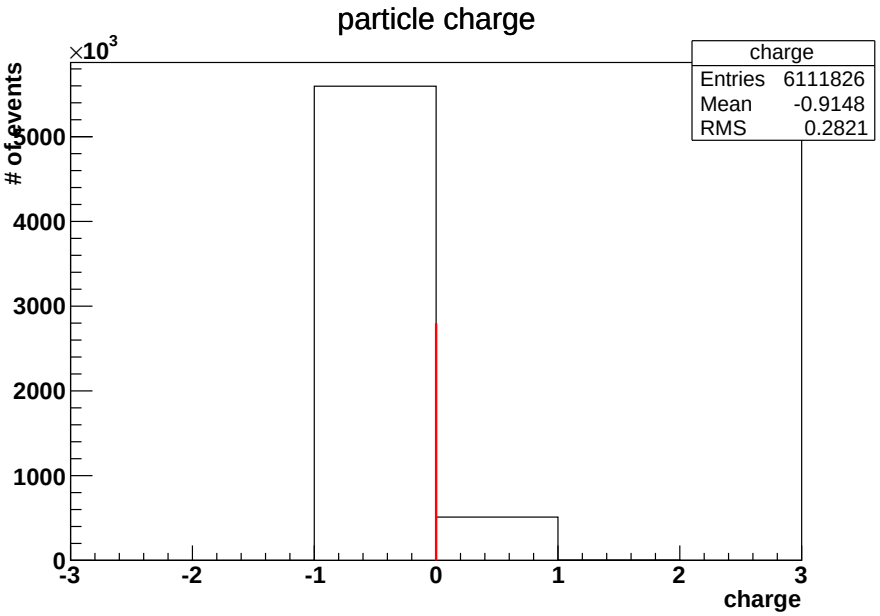

Figure 9: Track Cluster Matching

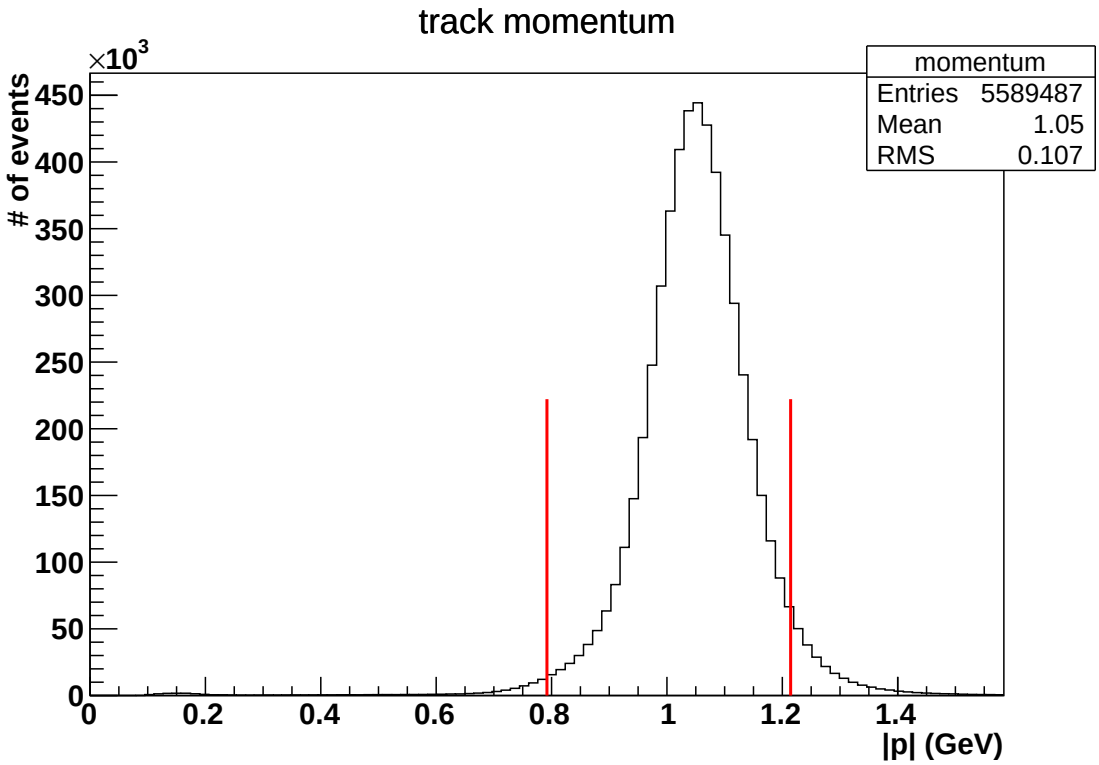

Figure 10: Track Momentum

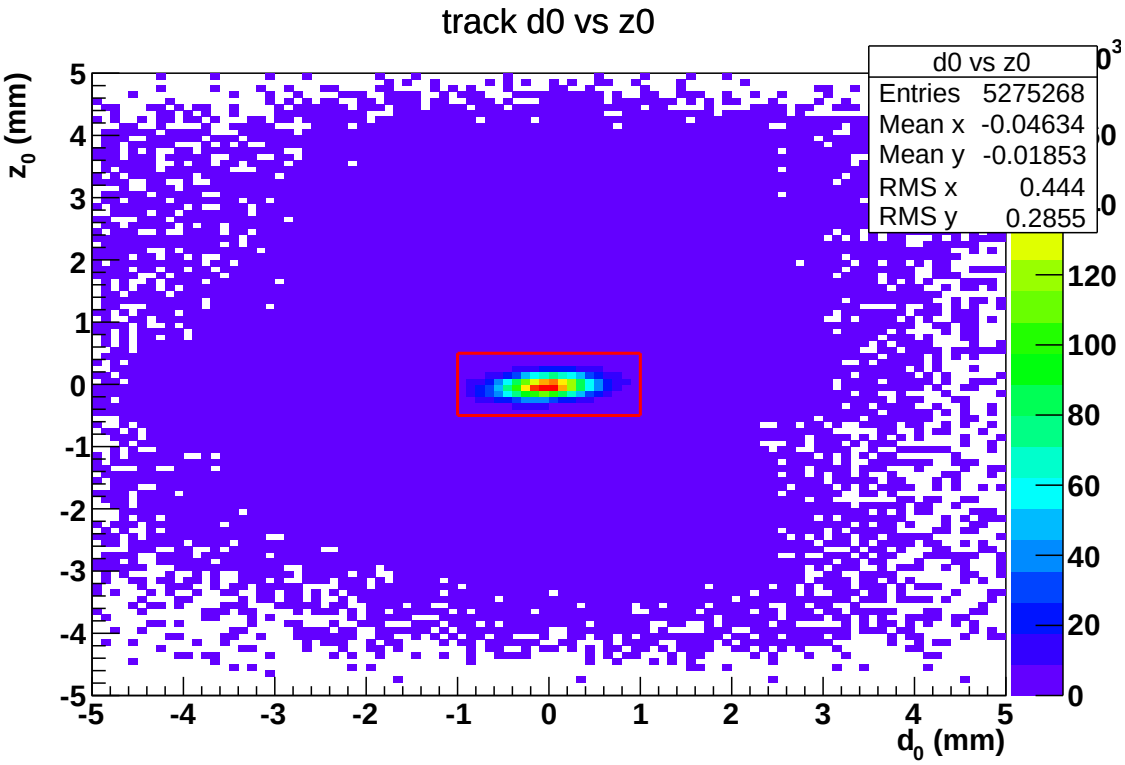

Figure 11: Track d0 and z0

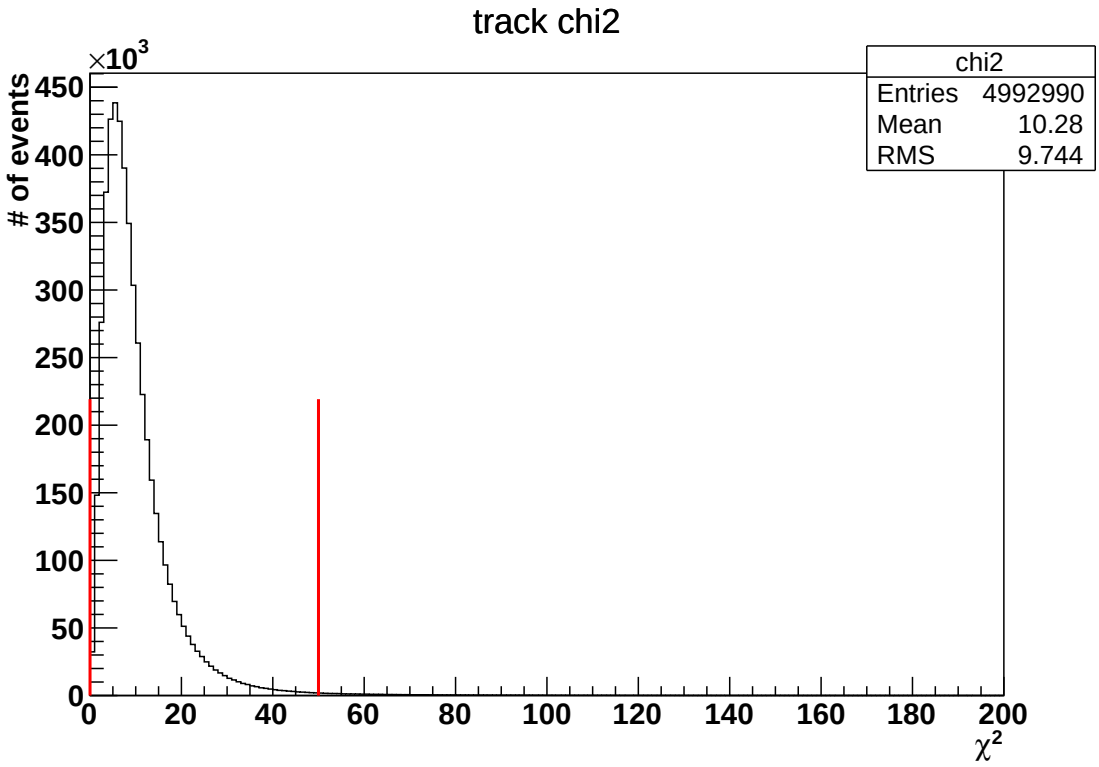

Figure 12: Track Chi Squared

8.3 Calculated Cross Section

Figure 13 shows the measured tungsten cross-section $\frac{d\sigma}{d\Omega}(\theta)$ as a fraction of the Mott scattering formula. This is calculated by taking the number of counts per bin from the tungsten runs, dividing by solid angle per bin, normalization factor, Mott formula, and the efficiency (as calculated using carbon). For comparison, I also include the a predicted form factor, in which I use the parameter values that Kalinsky et al fit their data from an earlier experiment [4].

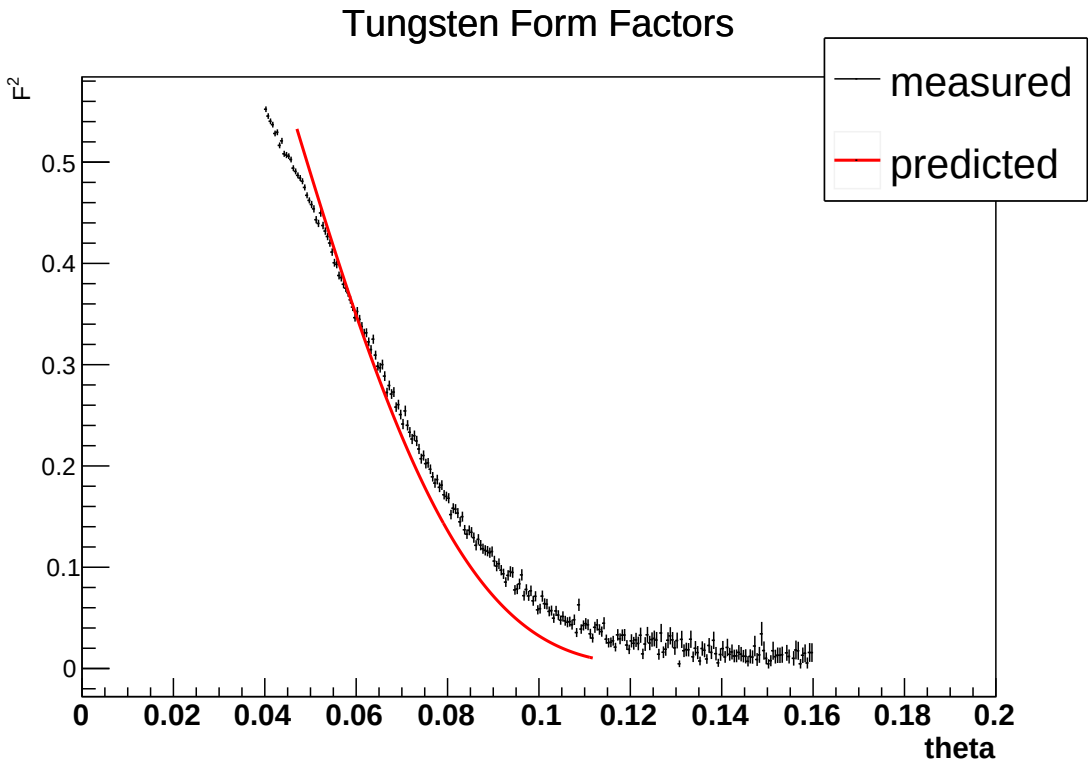

Figure 13: FEE cross section of tungsten as a fraction of the Mott cross section. The red curve represents the prediction using the parameters in [4].

9 To Do List for Future Studies

- The cut on seed hit energy (currently 400 MeV) needs to be loosened. When an FEE hits the Ecal in the center of a crystal, there is a large probablity of it passing this

cut. However, when the FEE hits the Ecal at the corner between 4 crystals, it is unlikely for it to pass the seed hit energy cut, because most of the energy will be spread out almost evenly between the 4 crystals.

- I have not taken into account the radiative corrections in the FEE model yet. This will need to be taken into account.
- When all of these things are ready and have been tested, I will increase the statistics by including all the runs in the sample.

A Prescale Factor

There was some controversy over whether the prescale factor is $2^{N-1}+1$ or 2^N, where the exponent N is the number specified in the trigger configuration file. It was discovered during the 2016 run that the prescale factor was $2^{N-1}+1$, however, it was not clear at the time if this was also the case during the 2015 run as well. To make this determination, I compared the data with singles1 trigger to the pulser data. After conversing with several of the trigger experts, it became clear that the 2^N prescale was used during the 2015 data. Figure 14 shows a comparison between the elastic peaks heights using single1 and pulsers, after normalizing them using the two different prescale factors.

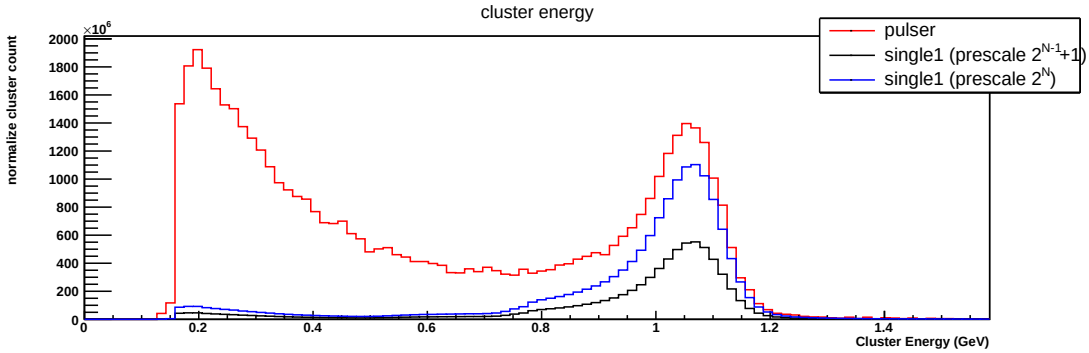

Figure 14: Comparison between the elastic peak height from pulsers versus singles1. The pulsers in the red curve are scaled by the time window of the pulsers divided by the pulser period. The blue and black curves represent the single1 events multiplied by 2^N and $2^{N-1}+1$ respectively. In each of these graphs, I used all the files in 5772 for consistency.

B Bibliography

References

[1] E. J. Moniz, I. Sick, R. R. Whitney, J. R. Ficenec, R. D. Kephart, and W. P. Trower, Phys. Rev. Lett. **26**, 445 (1971), URL `http://link.aps.org/doi/10.1103/PhysRevLett.26.445`.

[2] J. J. Kelly, Phys. Rev. **C70**, 068202 (2004).

[3] H. De Vries, C. W. De Jager, and C. De Vries, Atom. Data Nucl. Data Tabl. **36**, 495 (1987).

[4] D. Kalinsky, L. S. Cardman, R. Yen, J. R. Legg, and C. K. Bockelman, Nucl. Phys. **A216**, 312 (1973).